Supplemental Figure Legends

Supplemental Figure 1. Characterization of lenalidomide-resistant MM cells. (**A**) Pictures of the 6 cell lines used in this study. The insets show higher-magnification images of KMS21 and KMS21R cells. Scale bar: 50 μm. (**B**) Cell viability assay of KMS34 and KMS34R cells in the presence of lenalidomide. The values were normalized to those of the negative control. **(C)**. Caspase activity in KMS34 and KMS34R cells in the presence of lenalidomide, as measured with a caspase3/7 assay kit. (**D**) Picture of the MM cells on FN-coated glasses. Scale bar: 100 μm. Blue: Hoechst 33342 indicating nucleus; Red: CD138-positive MM cells. (**E**) Picture of the MM cells co-cultured with BMSCs. Scale bar: 50 μm. Blue: Hoechst 33342 indicating nucleus; Red: CD138-positive MM cells. CD138-negative cells are considered as BMSCs. **(F)** The adherent cell numbers in the FN-coated or BMSC-cocultured. *, $p<0.05$.

Supplemental Figure 2. Enriched pathways in lenalidomide-resistant cell lines. (**A**) GSEA (resistant (KMS21R and KMS27R) vs. parental (KMS27 and KMS21)) results showing the significantly enriched pathways in resistant cell lines. NES: normalized enrichment score. (**B**) A heatmap of the cell adhesion-related genes highly expressed in resistant cells. **(C)** A heatmap of the JAK/STAT pathway-related genes highly expressed in resistant cells.

Supplemental Figure 3. Characterization of MM cell-derived EVs. (**A**) Nanoparticle tracking analysis showing the particle size of MM cell-derived EVs. The vertical axis in the graphs shows the number of EVs ($\times 10^8$)/mL, and the horizontal axis indicates the particle size (nm) of EVs. (**B**) Western blot analysis of the typical EV marker proteins in MM cell-derived EVs. The proteins were loaded at 500 ng/lane.

Supplemental Figure 4. Coculture of parental cells with resistant cells. (**A**) Cell viability assay in parental cells. The values were normalized to those of the negative control. The error bars indicate the s.d. values. *, $p<0.05$. Parental cells (KMS21, KMS27) were cocultured with KMS21R and KMS27R cells. **(B)** The number of the adherent cells

after co-culture. *, $p < 0.05$. (**C**) KMS21 and KMS27 cell lines co-cultured with EV-depleted conditioned medium from each resistant cell line.

Supplemental Figure 5. Pathway analysis of resistant MM cell lines. (**A**) Illustration of activated pathways in the resistant cells, generated by IPA software. The orange nodes indicate activated pathways and the blue nodes indicate inhibited pathways in resistant MM cells. (**B**) Lists of upstream analysis data. Red bars: upregulated, blue bars: downregulated. Downregulated genes downstream (such as IKZF3 and IKZF1) of CRBN, lenalidomide-targeted genes, are marked in red. (**C**) Heat map showing the expression patterns of the lenalidomide-affected genes.

Supplemental Figure 6. The relationship of CRBN and LAMP2, SORT1. (A) public data and **(B)** our samples. **(C)** The protein levels of CRBN after knockdown of CRBN. **(D)** The quantification of the protein levels of CRBN. **(E)** The morphology of KMS27R cells after CRBN knockdown. Scale bar shows 50 μm. Bar graph shows the adherent cell numbers. $p<0.05$.

Supplemental Figure 7. Characterization of cells with shRNA-mediated knockdown of LAMP2 and SORT1. (**A**) Pictures of lenalidomide-resistant cells after knockdown of LAMP2 or SORT1. Scale bar: 50 μm. (**B**) Cell viability assay of KMS21R cells with LAMP2 or SORT1 knockdown in the presence of lenalidomide. The values were normalized to those of the negative control (0 μM lenalidomide). The error bars indicate the s.d. values. *, $p<0.05$. top; normal plate, bottom; FN-coated plate. (**C**) Western blotting of CRBN, VLA-4, STAT3, p-STAT3, β-actin, after silencing of LAMP2 and SORT1 genes. Protein was loaded at 15 μg/lane. (**D**) The expression level of CRBN after silencing LAMP2 and SORT1 genes. (**E**) Cell viability assay of KMS27R cells after LAMP2 or SORT1 knockdown in normal plates or ultra-low attachment plates. The black bars show the results for the normal plates, and the gray bars show the results for the ultra-low attachment plates.

Supplemental Figure 8. Value of EV secretion- and cell adhesion-related genes for

the prediction of MM patient prognosis. (**A**) UMAP plot classifying the patients. Each cluster indicates a different set of MM patients. BM: derived from bone marrow, EM: derived from extramedullary sites. (**B**) Principal component analysis of the 6 cell lines used in this study. The X-axis indicates the contribution of PC1, and the Y-axis indicates the contribution of PC2. (**C**) Top 50 genes in the PC1 and PC2 signatures.

Supplemental Figure 9. Violin plots of PC2 signature genes among patient states. *, $p<0.05$, **, $p<0.01$, ***, $p<0.001$

Supplementary Figure 1, Yamamoto T et al.

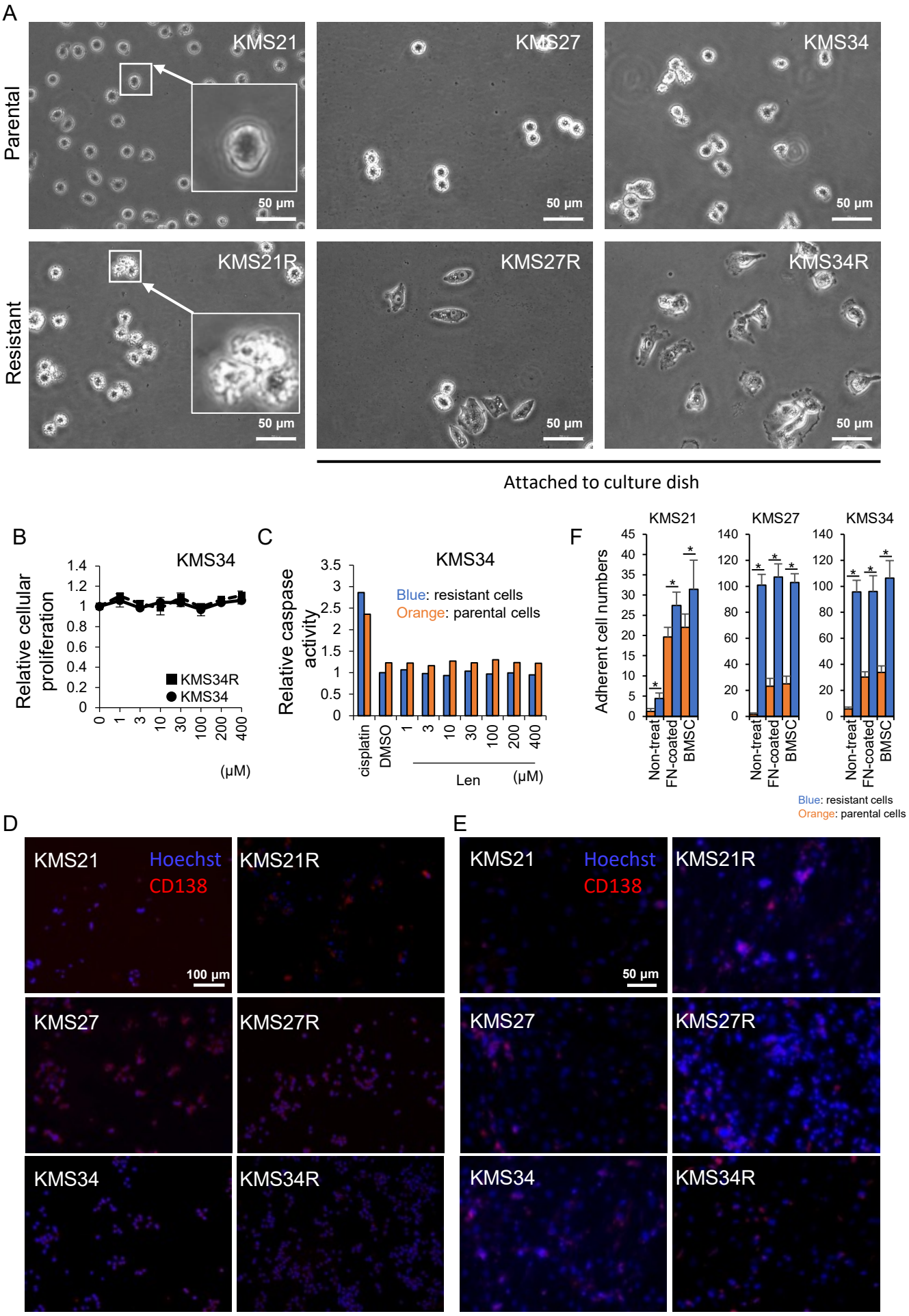

Supplementary Figure 2, Yamamoto T et al.

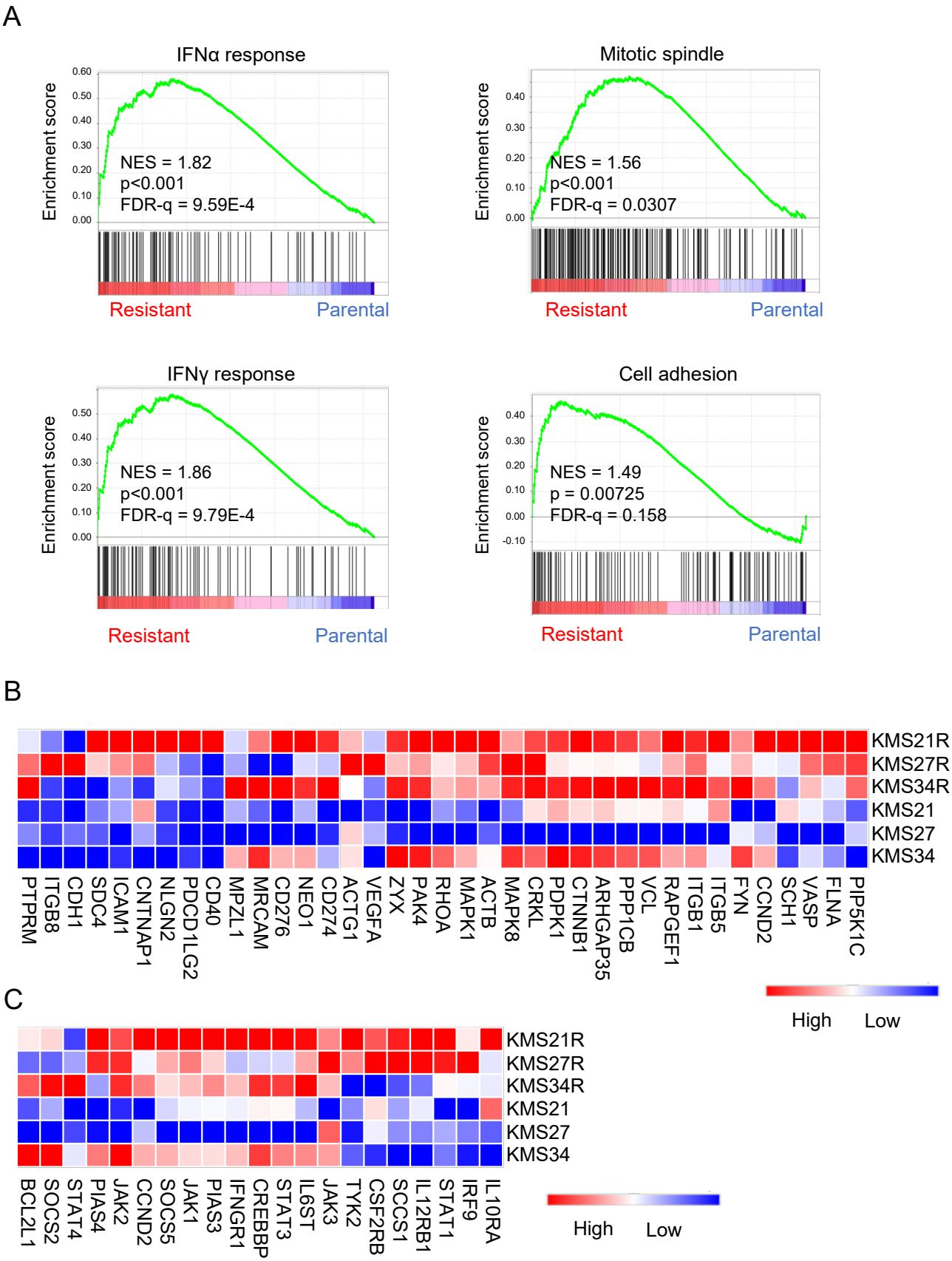

Supplementary Figure 3, Yamamoto T et al.

A

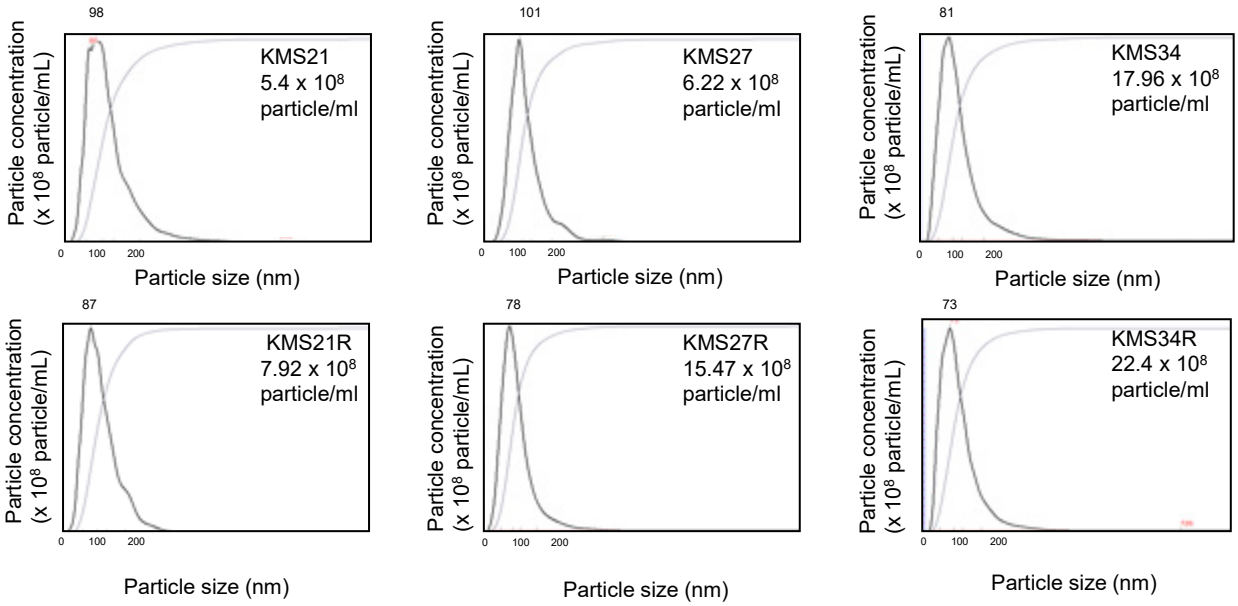

B

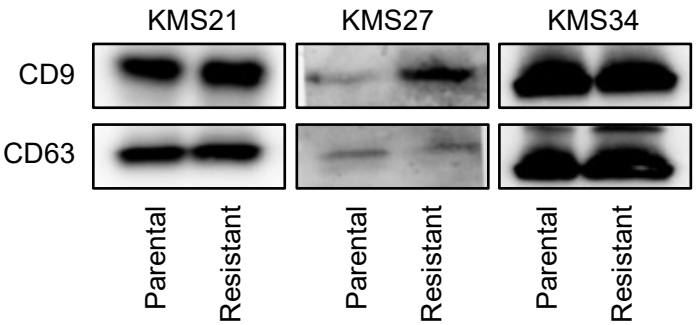

Supplementary Figure 4, Yamamoto T et al.

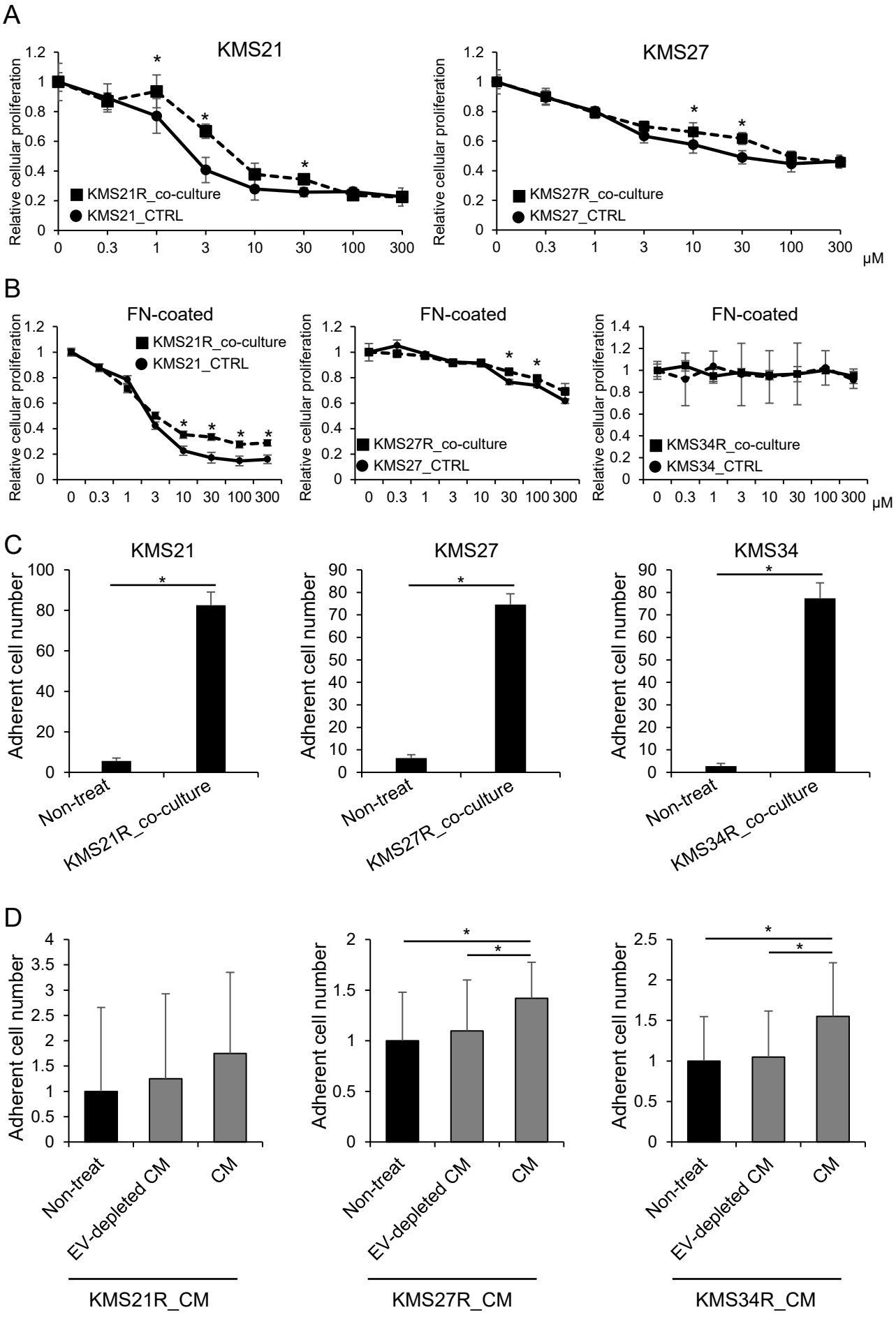

Supplementary Figure 5, Yamamoto T et al.

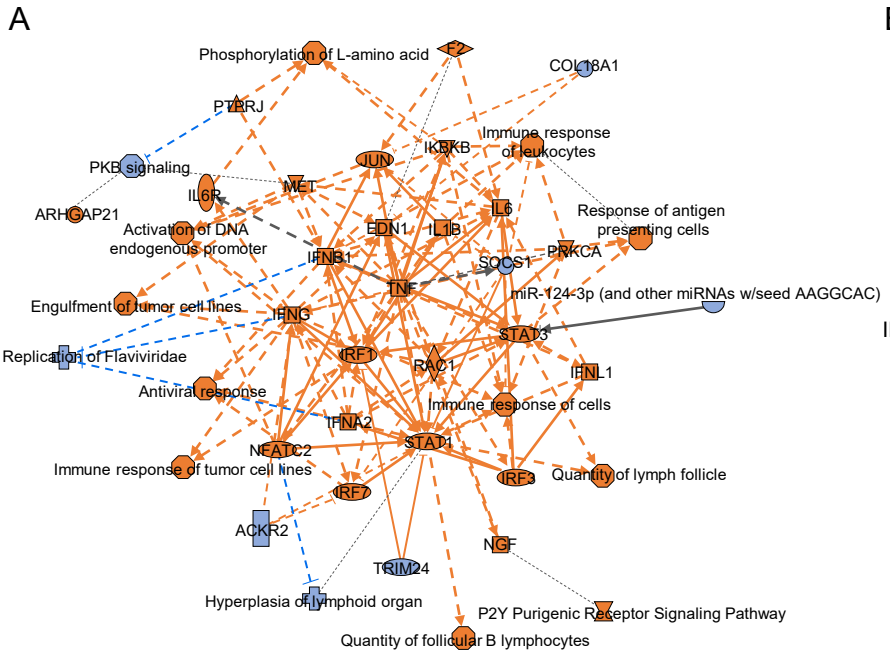

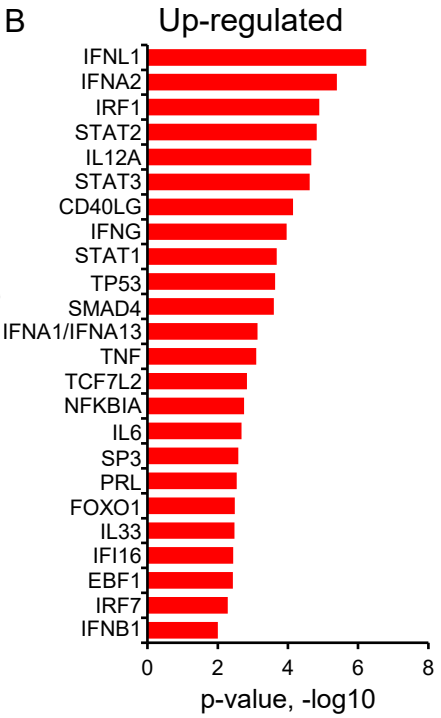

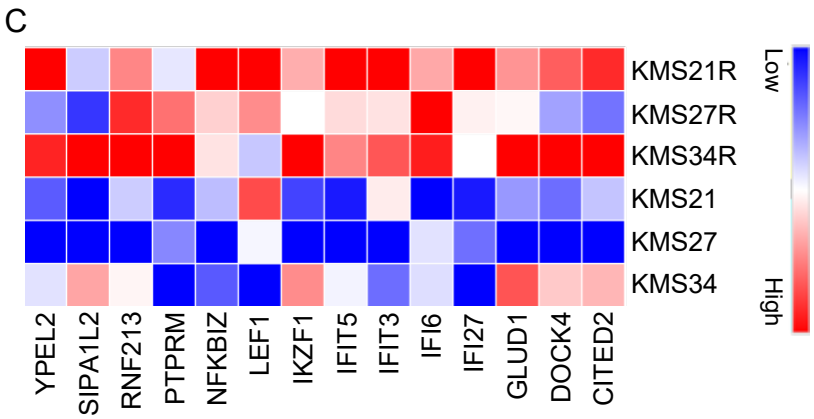

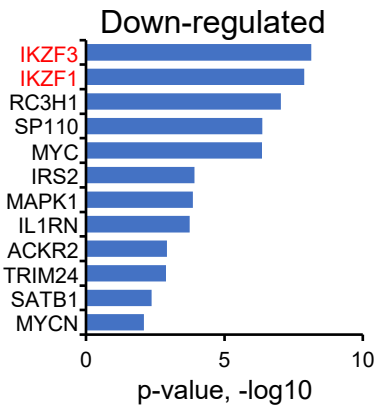

Supplementary Figure 6, Yamamoto T et al.

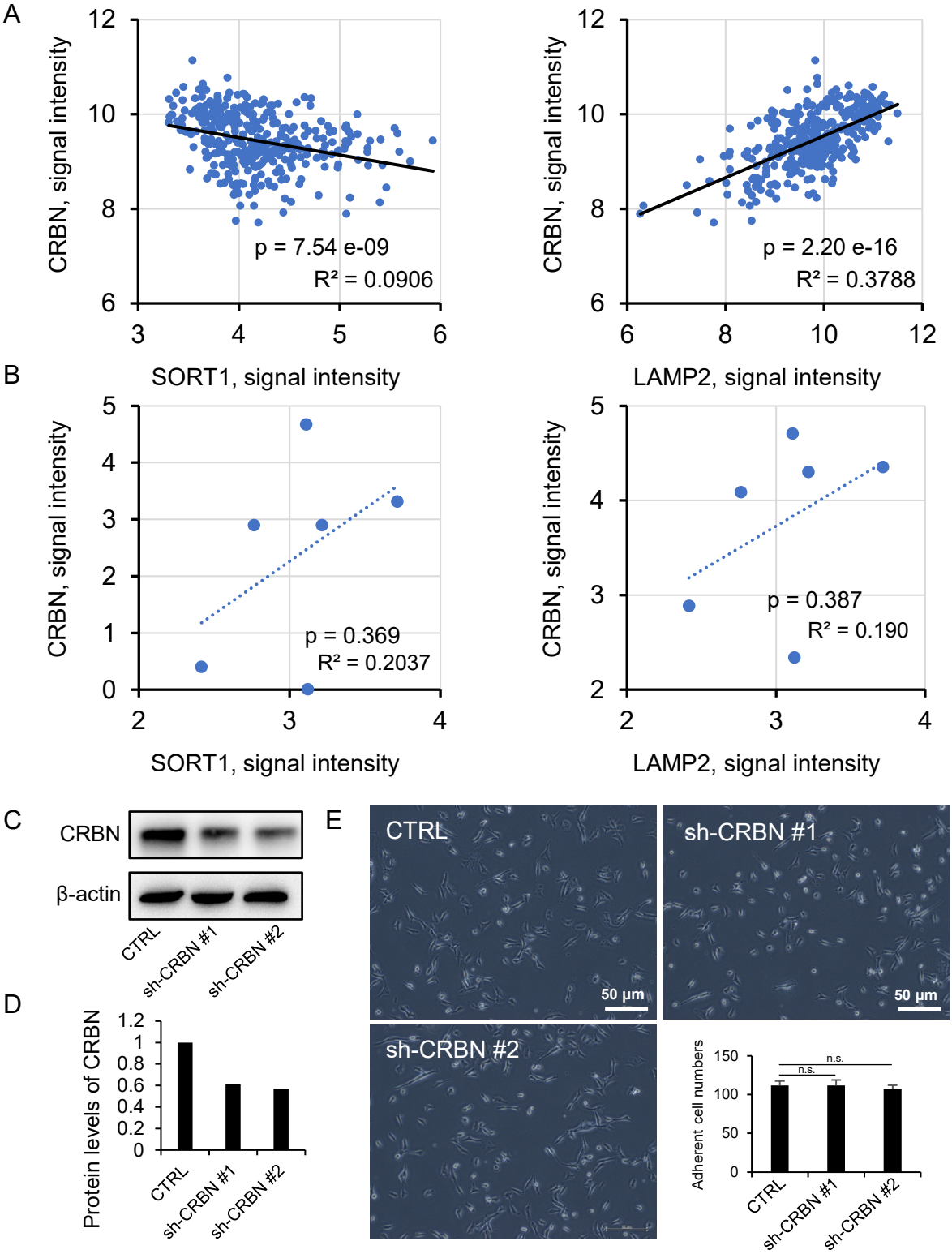

Supplementary Figure 7, Yamamoto T et al.

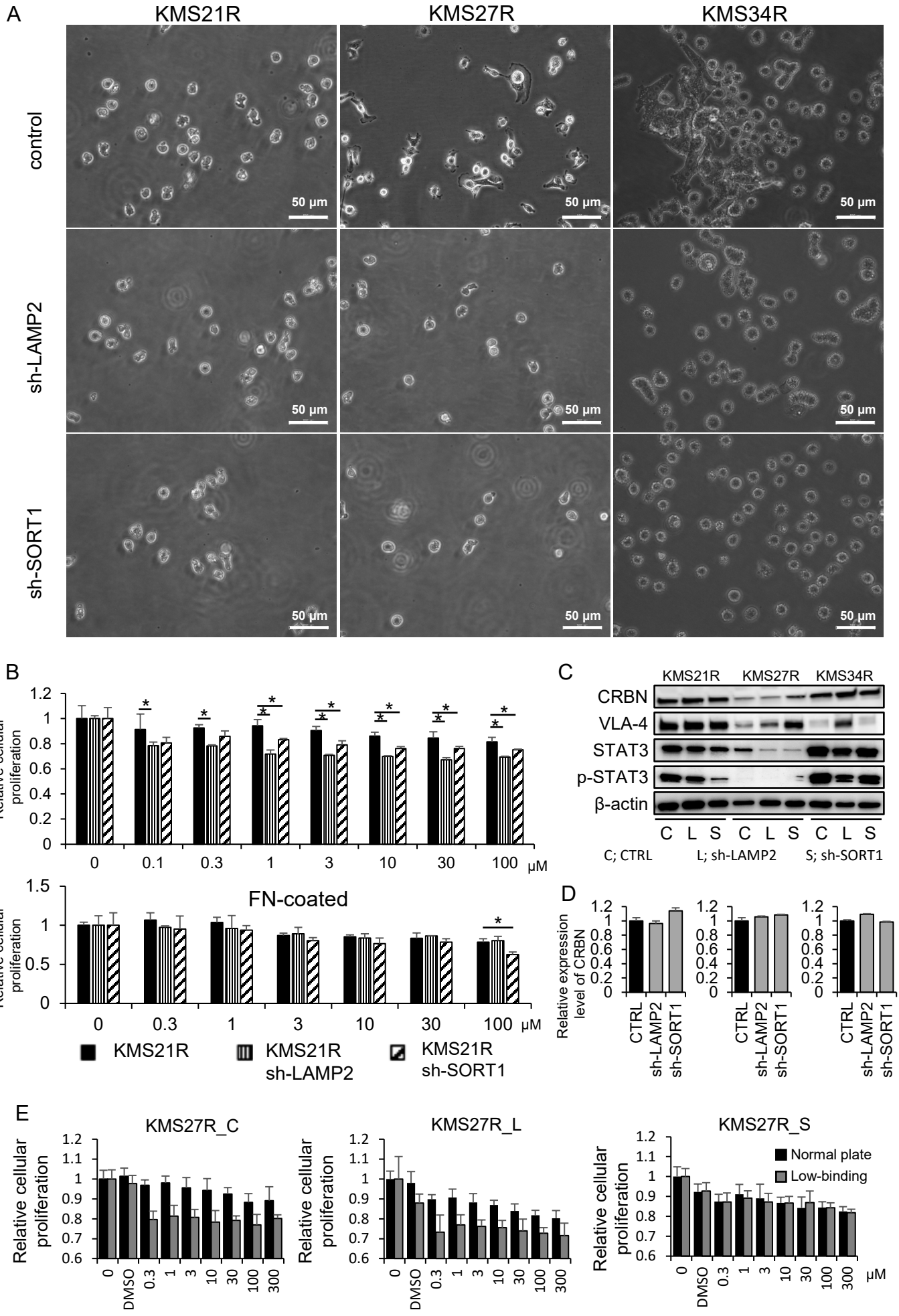

Supplementary Figure 8, Yamamoto T et al.

A

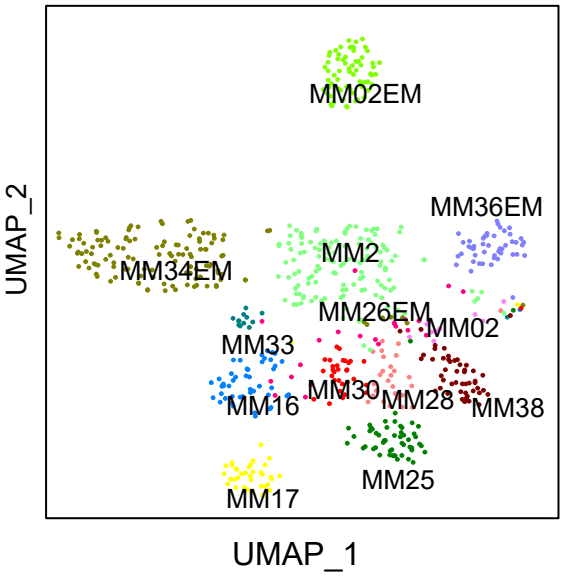

B

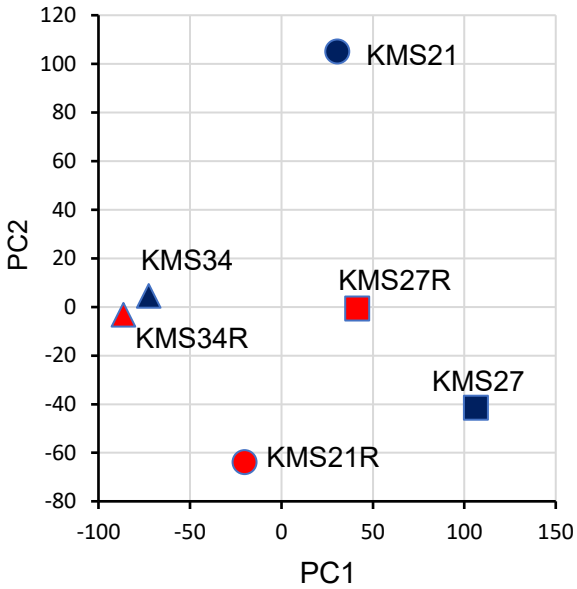

C

PC1_signature gene	CGB7	PEG3-AS1	CELP	NOS1	CHL1
	CLDN22	PHYHIPL	ECE2	DCHS2	PDE11A
	CYP2A6	PKD2L2	PCNA-AS1	SLC1A2	SHC3
	FUT6	PLGLA	OCM	LAMA3	GPR26
	KCNIP4	RIMS4	LOC440895	PTGER3	PRAMEF14
	LYPD1	SPATA22	USP17L5	GABRA4	FBN3
	NBPF14	SPRR2B	GRIN2B	CR1	COL6A5
	OR1E1	SPRR2E	TMEM155	MXRA5	ADAM12
	OR2T12	TP53TG5	LONRF2	NCR3	KCNK10
	PCDHB8	TSSK2	MUC21	ADAMTS5	PARVA
PC2_signature gene	ITM2C	EYA2	TMSB15A	SULF1	PFKP
	CTHRC1	ITM2A	CAV1	JUP	IGF2BP3
	CD9	PTP4A3	FGFR3	FUCA2	CD44
	HES6	CA2	GPAT2	TSPAN7	RASSF4
	ANXA1	PEG10	CDH2	TUBB3	PFN2
	IDH2	AHNAK	TUBB2B	LRIG1	DSG2
	ITGB7	GPRC5D	CYB5A	CLU	MAF
	GAS6	MEST	PLD4	TMEM173	AP1S2
	MCAM	AGT	CST3	PDLIM1	PDE3B
	MARCKSL1	PTPRCAP	RCN1	TIMP2	SLC16A14

Supplementary Figure 9, Yamamoto T et al.